



Factors affecting B/Ca ratios in synthetic aragonite



M. Holcomb^{a,b,c,*}, T.M. DeCarlo^d, G.A. Gaetani^e, M. McCulloch^{a,b}

^a The UWA Oceans Institute and School of Earth and Environment, The University of Western Australia, Crawley 6009, WA, Australia

^b ARC Centre of Excellence in Coral Reef Studies, The University of Western Australia, Crawley 6009, WA, Australia

^c Centre Scientifique de Monaco, Principality of Monaco, Monaco

^d Massachusetts Institute of Technology/Woods Hole Oceanographic Institution Joint Program in Oceanography/Applied Ocean Physics and Department of Marine Geology and Geophysics, Woods Hole, MA 02543, USA

^e Woods Hole Oceanographic Institution, Department of Marine Geology and Geophysics, Woods Hole, MA 02543, USA

ARTICLE INFO

Article history:

Received 14 September 2015

Received in revised form 1 May 2016

Accepted 9 May 2016

Available online 11 May 2016

Keywords:

Boron

Aragonite

Coral

Proxy

Carbonate

ABSTRACT

Measurements of B/Ca ratios in marine carbonates have been suggested to record seawater carbonate chemistry, however experimental calibration of such proxies based on inorganic partitioning remains limited. Here we conducted a series of synthetic aragonite precipitation experiments to evaluate the factors influencing the partitioning of B/Ca between aragonite and seawater. Our results indicate that the B/Ca ratio of synthetic aragonites depends primarily on the relative concentrations of borate and carbonate ions in the solution from which the aragonite precipitates; not on bicarbonate concentration as has been previously suggested. The influence of temperature was not significant over the range investigated (20–40 °C), however, partitioning may be influenced by saturation state (and/or growth rate). Based on our experimental results, we suggest that aragonite B/Ca ratios can be utilized as a proxy of $[\text{CO}_3^{2-}]$. Boron isotopic composition ($\delta^{11}\text{B}$) is an established pH proxy, thus B/Ca and $\delta^{11}\text{B}$ together allow the full carbonate chemistry of the solution from which the aragonite precipitated to be calculated. To the extent that aragonite precipitation by marine organisms is affected by seawater chemistry, B/Ca may also prove useful in reconstructing seawater chemistry. A simplified boron purification protocol based on amberlite resin and the organic buffer TRIS is also described.

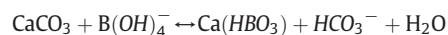
© 2016 Elsevier B.V. All rights reserved.

1. Introduction

Boron concentrations and boron isotopic compositions in marine carbonates are potential archives of past seawater pH and carbonate chemistry (e.g. Sanyal et al., 1996; Pelejero et al., 2005; Pearson and Palmer, 1999; Douville et al., 2010; Rae et al., 2011; Henehan et al., 2013; Penman et al., 2013). In seawater, boron is typically present in two forms, boric acid $\text{B}(\text{OH})_3$ and borate $\text{B}(\text{OH})_4^-$, the relative abundances of which depend largely on pH (e.g. Culberson and Pytkowicz, 1968; Dickson, 1990; Klochko et al., 2006). The $\text{B}(\text{OH})_4^-$ ion is thought to be the primary form of boron incorporated into calcium carbonate (e.g. Sen et al., 1994; Hemming et al., 1995), thus offering the potential to use B/Ca ratios to estimate pH and/or carbonate chemistry (e.g. Yu et al., 2007). However, there is uncertainty as to how boron incorporation may depend upon concentrations of different dissolved inorganic carbon (DIC) species (e.g. Hemming et al., 1995; Uchikawa et al., 2015). In addition, there are suggestions that $\text{B}(\text{OH})_3$ may also be incorporated, especially in calcite (e.g. Xiao et al., 2008; Klochko et al., 2009; Rollion-Bard et al., 2011; Mavromatis et al., 2015; Uchikawa et al., 2015), thus potentially complicating the interpretation of B/Ca ratios.

Various relationships have been used to explore the range of possible factors controlling B incorporation in both synthetic (e.g. Mavromatis et al., 2015; Uchikawa et al., 2015) and biogenic carbonates (e.g. Ni et al., 2007; Yu et al., 2007; Yu and Elderfield, 2007; Foster, 2008; Douville et al., 2010; Allen et al., 2011; Rae et al., 2011; Tripati et al., 2011; Allen et al., 2012; Allison et al., 2014; Babila et al., 2014; Henehan et al., 2015). Here we consider several of the relationships proposed by previous studies: $\text{B}(\text{OH})_4^-/\text{CO}_3^{2-}$, $\text{B}(\text{OH})_4^-/\text{HCO}_3^-$, $\text{B}(\text{OH})_4^-/(\text{CO}_3^{2-} + \text{HCO}_3^-)$, B/HCO_3^- , $\text{B}/(\text{CO}_3^{2-} + \text{HCO}_3^-)$, $\text{B}(\text{OH})_4^-/\Delta\text{CO}_3^{2-}$ (where ΔCO_3^{2-} is the difference between the actual $[\text{CO}_3^{2-}]$ and the $[\text{CO}_3^{2-}]$ at which the solution would be saturated with respect to aragonite, $\Omega_{\text{Arag}} = 1$). In addition to various empirical relationships, we also consider potential balanced exchange reactions with the following expressions for the distribution coefficient:

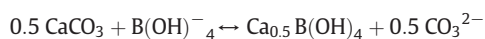
Reaction (1) (Hemming and Hanson, 1992):



$$K_D = \frac{[\text{HBO}_3^-/\text{CO}_3^{2-}]_{\text{CaCO}_3}}{[\text{B}(\text{OH})_4^-/\text{HCO}_3^-]_{\text{solution}}} \quad (1)$$

Reaction (2):

* Corresponding author at: The UWA Oceans Institute and School of Earth and Environment, The University of Western Australia, Crawley 6009, WA, Australia.
E-mail address: mholcomb3051@gmail.com (M. Holcomb).



$$K_D = \frac{[\text{B(OH)}_4^- / [\text{CO}_3^{2-}]^{0.5}]_{\text{CaCO}_3}}{[\text{B(OH)}_4^- / [\text{CO}_3^{2-}]^{0.5}]_{\text{solution}}} \quad (2)$$

Reaction (3):



$$K_D = \frac{[[\text{BO}_3^{3-}]^2 / [\text{CO}_2]^{0.5}]_{\text{CaCO}_3}}{[[\text{B(OH)}_4^-]^2 / [\text{CO}_2][\text{HCO}_3^-]^2]_{\text{solution}}} \quad (3)$$

Studies of naturally formed samples do provide some insights into the potential controls on boron incorporation (Hemming and Hanson, 1992; Sanyal et al., 1996; Wara et al., 2003; Ni et al., 2007; Yu et al., 2007; Yu and Elderfield, 2007; Foster, 2008; Rollion-Bard et al., 2011; Allison et al., 2014; Kaczmarek et al., 2015). However, such studies cannot establish how B/Ca is controlled by environmental variables due to inevitable uncertainty as to the conditions during carbonate deposition. This is particularly the case for calcifying organisms that modify the conditions at the site of calcification substantially from the conditions present in the surrounding seawater (e.g. Al-Horani et al., 2003; McCulloch et al., 2012; De Nooijer et al., 2014). Since the chemistry at the site of calcification is generally unknown, most studies have focused on the relationship between B/Ca and seawater chemistry. Thus in studies of biologically formed calcium carbonate, there is uncertainty as to whether B/Ca changes in direct response to environmental conditions, or if it reflects physiological changes in the organism.

Laboratory studies on the incorporation of B into calcium carbonate remain limited, and few potentially controlling factors (e.g. temperature, carbonate chemistry, and growth rate) have been tested (Kitano et al., 1978; Sen et al., 1994; Hemming et al., 1995; Hobbs and Reardon, 1999; Sanyal et al., 2000; Xiao et al., 2008; He et al., 2013; Gabitov et al., 2014; Mavromatis et al., 2015; Uchikawa et al., 2015). Critically only one study has characterized the carbonate chemistry during aragonite precipitation (Mavromatis et al., 2015).

We conducted a series of experiments to explore how carbonate chemistry, organic additives, temperature, and boron concentration may influence B/Ca ratios in aragonite formed from seawater-like solutions. Manipulation of pH, DIC, and Ca^{2+} are among the mechanisms potentially driving biogenic calcification, thus our experiments focused on manipulating these variables. In addition to these inorganic variables, there are also a wide range of organic molecules produced by calcifying organisms which may influence calcification (e.g. Mass et al., 2013). We chose to test one specific mechanism by which organic molecules could influence B/Ca, that of buffering pH. In seawater, the two dominant pH buffers are DIC and B species, thus variations in pH (such as might occur adjacent to a growing aragonite crystal) would directly affect DIC and B speciation. By adding an additional buffering agent (such as 2-amino-2-hydroxymethyl-propane-1,3-diol (TRIS) or 4-(2-hydroxyethyl)-1-piperazineethanesulfonic acid (HEPES)), pH could in theory be more stable adjacent to the growing crystal which could alter the relationship between B/Ca and bulk solution chemistry. In addition to biological processes affecting elemental ratios, there is also a potential for some of the compounds used to study crystal growth to influence elemental incorporation. Calcein is among the molecules commonly used to mark growing crystals in living organisms (e.g. Venn et al., 2013), and the influence of calcein on the incorporation of a number of elements has been tested (Dissard et al., 2009), though no information is thus far available as the effect of calcein on B/Ca, thus it was tested here.

2. Methods

2.1. Aragonite precipitation

Aragonite was precipitated from seawater (0.2 μm filtered to remove living organisms) using several different approaches adapted from existing methods (Kinsman and Holland, 1969; Kitano et al., 1978; Gaetani and Cohen, 2006; Holcomb et al., 2009; Gabitov et al., 2011; Wang et al., 2013). The range of experimental protocols used was intended to precipitate aragonite under a wide range of solution chemistries in order to encompass the likely compositional range of biologically mediated solutions and thus more fully evaluate the factors that affect boron incorporation during bio-calcification. Detailed descriptions of the protocols used for each of the 65 experiments are provided in the Supplementary materials (see section S1 and Table S1 for more details). Briefly, all experiments were carried out in plastic containers held within constant temperature water baths. Two general types of experiments were conducted: degassing (Fig. 1B) and pumping (Fig. 1A) experiments. Degassing experiments were carried out by dissolving CaCO_3 in seawater at ~ 1 atm pCO_2 with the addition of MgCl_2 , SrCO_3 (to maintain seawater like Mg/Ca and Sr/Ca ratios) and various additives (TRIS, HEPES, calcein, boron, CaCl_2 , etc. depending upon the experiment). As CO_2 degassed in these experiments, Ω_{Arag} increased until aragonite began to precipitate. Degassing experiments were bubbled at controlled rates with air or air/ CO_2 mixes during precipitation to stabilize pH. Pumping experiments were conducted by adding seawater containing CaCO_3 (dissolved by bubbling with CO_2) or concentrated seawater (evaporated to achieve $2 \times$ normal salinity = $2 \times$ sw) and a NaHCO_3 or Na_2CO_3 or NaOH or mixture thereof solution (here after referred to as NaX solution) to seawater using a syringe pump. The simultaneous injection of $2 \times$ sw and NaX solutions allowed carbonate chemistry to be modified while maintaining salinity \sim constant. Pumping rates were varied over the course of each experiment to stabilize pH during precipitation. Some of these experiments were additionally bubbled with air or air/ CO_2 mixtures, and some contained additional additives. All experiments were stirred continuously.

The evolution of solution chemistry during precipitation differed among experiments. In general, in pumping experiments an initial pH and alkalinity was established, precipitation then removed CO_3^{2-} thus reducing DIC (or equivalently total inorganic carbon) and alkalinity, while pumping of the NaX solution added DIC and alkalinity, thus allowing carbonate chemistry to be maintained nearly constant during precipitation. In degassing experiments, though pH was maintained nearly constant, DIC, and alkalinity both declined during precipitation due to the precipitate removing DIC and alkalinity and bubbling removing DIC. To illustrate the relationships between different solution chemistry parameters potentially relevant for B/Ca, Fig. 2 shows various chemical parameters plotted versus pH_T for our experiments, as well as the values expected for seawater at different DIC concentrations.

Over the course of each experiment, samples were taken for pH, alkalinity, and solution chemistry measurements. Samples for alkalinity and solution chemistry were filtered (Millex-HV syringe filter, 0.45 μm PVDF membrane) at the time of collection to remove any aragonite particles potentially present. All seawater samples used for elemental composition measurements were acidified with concentrated HNO_3 to dissolve any material that precipitated post-collection. Details of all measurements, associated calculations, and measured values are provided in the supplementary materials (Sections S2, S3, and .xls file).

2.2. Precipitate characterization

2.2.1. Mineralogy

The mineralogy of most experiments was characterized by XRD (see Supplemental materials section S4) and/or Raman spectroscopy (DeCarlo et al., 2015; and Supplemental materials S4). Some experiments contained phases other than aragonite and were generally

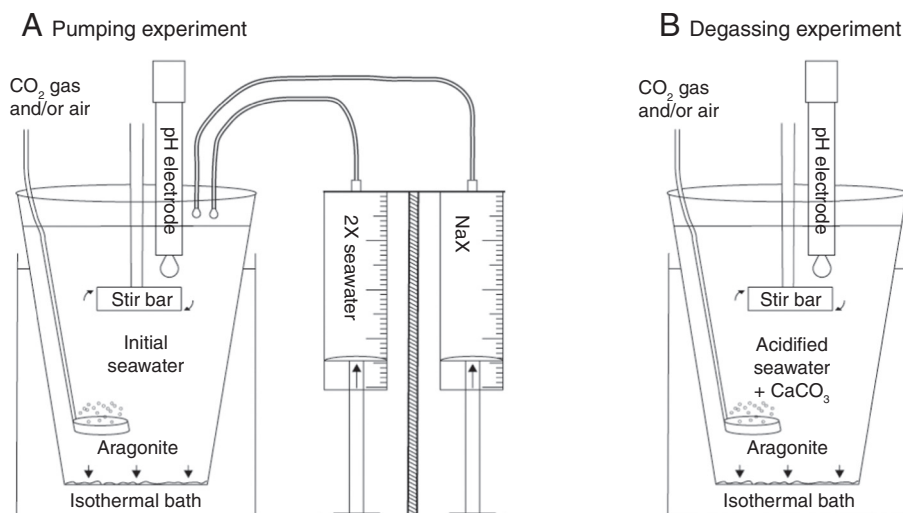


Fig. 1. Schematic representation of the experimental setup used for pumping (A) and degassing (B) experiments.

excluded from analysis of B/Ca, with the exception of one sample (10 h) which had a faint XRD peak near $2\text{-}\theta = 30$, suggesting possible contamination with a calcitic phase, but neither the Raman spectra nor the elemental composition indicated a non-aragonitic phase, thus any contamination was assumed to be sufficiently low as to not compromise the use of the sample.

2.2.2. Composition

The elemental composition of all precipitates was measured using Q-ICPMS (Supplemental materials S3.1) to verify that the elemental composition was similar to other marine aragonite samples while simultaneously measuring the B/Ca ratio. The coral standard JCp-1 (B/Ca = 0.4596 mmol/mol, Hathorne et al. (2013)) was used to standardize all measurements, and the validity of this approach for measuring B/Ca was verified using independent measurements of purified boron extracts measured via MC-ICPMS (Supplemental materials S3.2.1). Data on the incorporation of Sr/Ca and U/Ca into these precipitates is published elsewhere (DeCarlo et al., 2015).

2.3. Solution characterization

Since natural seawater was used for all experiments, and Ca and B are generally considered uniformly distributed throughout the oceans in proportion to salinity, concentrations were calculated based on salinity and the mass of any added B- or Ca-containing solutions. For a subset of experiments the validity of this assumption was verified via ICP-MS measurements. Measurements are described in the supplemental materials including the description of new simplified chemistry for the purification of boron based on amberlite IRA 743 resin and the organic buffer TRIS (Supplemental material S3.3).

2.4. Calculations

Carbonate chemistry was calculated using the measured alkalinity, pH, and temperature. When pH measurements were carried out at a temperature different from that of the experimental temperature, the pH at the experimental temperature was calculated using CO2Sys (van Heuven et al., 2009). Salinities were interpolated based on initial and final salinities and estimated evaporation rates. Calcium and boron concentrations in the fluid were calculated based on salinity, estimated amount of precipitate deposited, and any calcium or boron added to the experiment. These experiments were undertaken in conjunction with those reported by DeCarlo et al. (2015), further details

are given in the Supplemental materials (S2), as are alternative calculations using constants from Hain et al. (2015) (S6).

Since aragonite is primarily CaCO_3 , and thus $\text{Ca} \approx \text{CO}_3$, B/Ca can be substituted for B/ CO_3 when calculating distribution coefficients, so though Eqs. (1)–(3) are expressed relative to CO_3 in the solid, B/Ca will be used for calculations.

2.5. Average solution chemistry and partitioning

We evaluated the factors controlling B incorporation into aragonite by comparing the bulk/mean aragonite B/Ca ratio to the average solution composition during precipitation of each of 58 experiments conducted in 2013 (of 65 total experiments). The solution chemistry and bulk precipitation rates varied over the course of each experiment. To estimate the average solution chemistry during the time that aragonite precipitated, chemistry parameters were weighted by the amount of precipitate formed over the given time interval (estimated from the difference between measured and expected alkalinity). The distribution coefficient relationship that best described the data was then used to calculate distribution coefficients for each individual experiment such that the calculated B/Ca ratio for the final precipitate in each experiment matched the measured ratio. Data from experiments run in 2011 (denoted by a '11' in the experiment name in the supplemental tables) were not included in these comparisons as carbonate chemistry was generally less stable; experiments from 2011 were used only for assessing the effects of calcin.

3. Results

Aragonite was precipitated over a wide range of pH_T (7.3 to 9.3, where pH_T is pH measured on the total scale), temperature (~ 20 °C to 40 °C), and carbonate chemistry conditions (Fig. 2). Within any given experiment, the precipitate formed under a range of solution chemistry conditions, but the range within an experiment was generally small relative to the differences among experiments (Fig. 2). For example, the within-experiment pH variation was typically < 0.1 pH units, whereas among experiments pH differences of > 2 pH units were achieved. Likewise, within the course of an experiment, the relative standard deviation (RSD) of $[\text{B}(\text{OH})_4^-]/[\text{CO}_3^{2-}]^{0.5}$ was $< 15\%$ (typically $< 5\%$), while different experiments differed by more than an order of magnitude (Fig. 2H, Table S2).

The B/Ca ratio in the precipitate showed no significant ($p > 0.05$) correlation with pH_T or any single carbonate chemistry parameter. Significant ($p < 0.001$) correlations were found between B/Ca and the mean

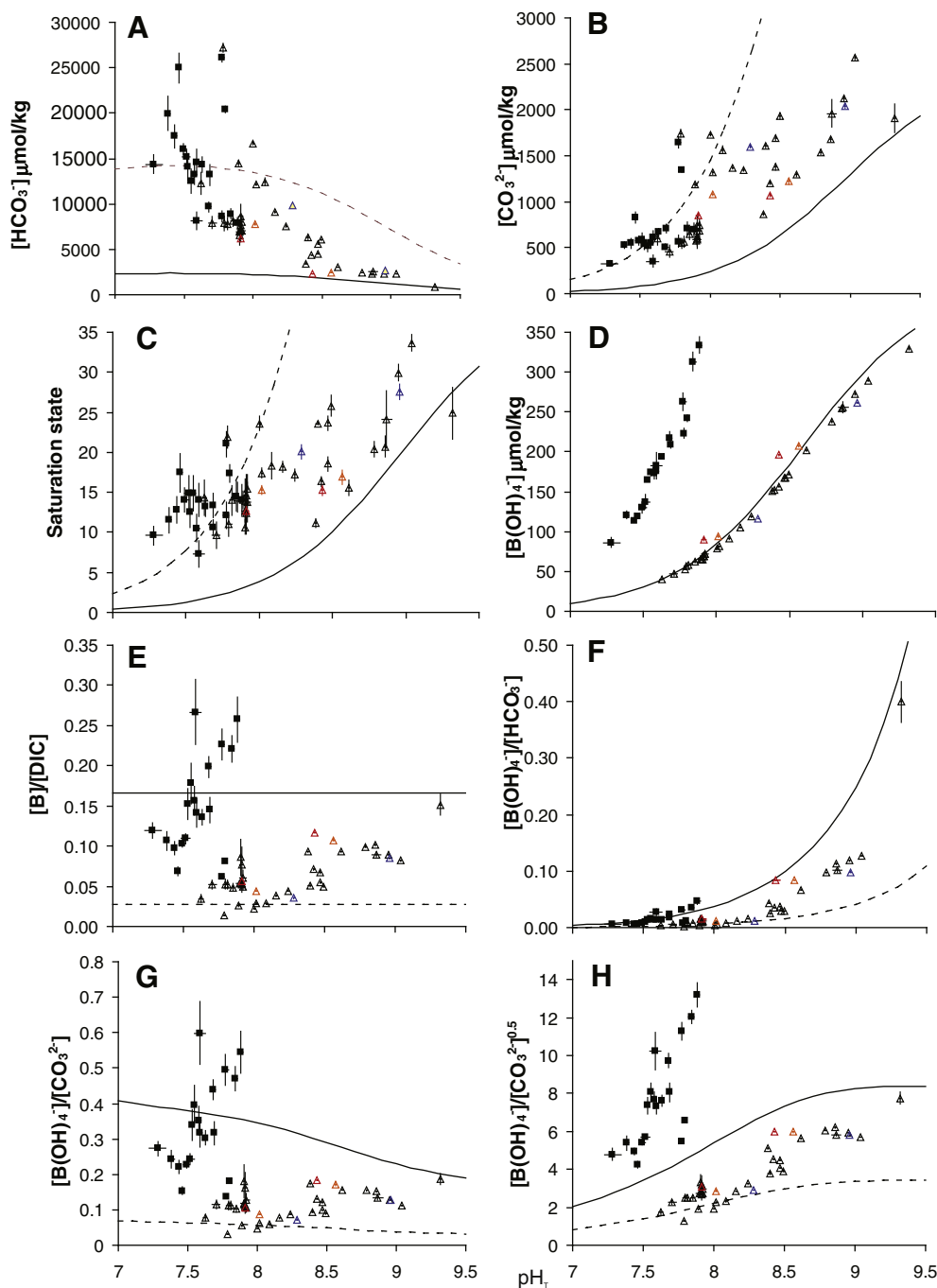


Fig. 2. Relationship between different solution chemistry parameters and pH_T (total scale pH). Symbols are means of individual experiments; experiments without added B are represented by triangles, experiments with added B are represented by squares, lines show bi-direction error bars (1 standard deviation (sd)). Experiments conducted at different temperatures are shown in different colors: blue ~20, black ~25, orange ~33, and red ~40 °C. Most experiments were conducted at ~25 °C, 2 experiments were run at each of the other temperatures. Lines show calculated concentrations of different DIC species and borate ($\mu\text{mol/kg}$ sw) as a function of seawater pH_T . Calculated values are for seawater ($S = 35$, $T = 25$ °C) with either 2500 (solid line) or 15,000 (dashed line) $\mu\text{mol DIC/kg}$ sw. (For interpretation of the references to color in this figure legend, the reader is referred to the web version of this article.)

solution [B] and $[\text{B}(\text{OH})_4^-]$ (Table 1). However, when considering only precipitates formed under seawater boron concentrations, B/Ca does correlate significantly with a number of carbonate system parameters, most notably pH and parameters closely correlated with pH (e.g. DIC species and $[\text{B}(\text{OH})_4^-]$; Fig. 3, Table 1), with $[\text{B}(\text{OH})_4^-]$ remaining the single parameter most strongly correlated with B/Ca.

Since boron is thought to compete with DIC species for incorporation into aragonite (e.g. Hemming and Hanson, 1992), correlations between precipitate B/Ca and various solution boron/DIC relationships were explored (Table 1). In the full data-set, B/Ca and mean $[\text{B}(\text{OH})_4^-]/[\text{HCO}_3^-]$ were not strongly correlated (Fig. 3b, based on Eq. (1)), nor were the

residuals of a $[\text{B}(\text{OH})_4^-]$ vs B/Ca regression and $[\text{HCO}_3^-]$. Nor was there a significant correlation between B/Ca and average $[\text{B}(\text{OH})_4^-]^2 / [\text{CO}_2][\text{HCO}_3^-]^2$ (Eq. (3)). B/Ca in the precipitate was most strongly correlated with the mean $[\text{B}(\text{OH})_4^-] / [\text{CO}_3^{2-}]^{0.5}$ (Eq. (2)), $[\text{B}]/[\text{DIC}]$ or $[\text{B}] / ([\text{CO}_3^{2-}] + [\text{HCO}_3^-])$ and $[\text{B}(\text{OH})_4^-] * [\text{Ca}^{2+}]$ (Table 1, Fig. 3). The correlations of B/Ca with $[\text{B}(\text{OH})_4^-] / [\text{CO}_3^{2-}]^{0.5}$ and $[\text{B}] / [\text{DIC}]$ or $[\text{B}] / ([\text{CO}_3^{2-}] + [\text{HCO}_3^-])$ were important regardless of whether B was added or whether only pumping or degassing experiments were considered. Conversely $[\text{B}(\text{OH})_4^-] * [\text{Ca}^{2+}]$, though significantly correlated with B/Ca, did not necessarily correlate more strongly than $[\text{B}(\text{OH})_4^-]$ alone (Table 1). When only a subset of the experiments is considered, some

Table 1

Pearson correlation coefficients for mean solution chemistry parameters showing the most significant correlations with the B/Ca ratio of the precipitate, as well as various proposed ratios suggested to be linked to B/Ca regardless of significance. Correlation coefficients are given for the data set as a whole ($n = 58$, excluding experiments run in 2011), for experiments without added B ($n = 39$), and for pumping experiments without added B ($n = 28$). Significant ($p < 0.05$) individual correlations are indicated by *.

| Species in solution | Correlation with precipitate B/Ca | | |
|--|-----------------------------------|-------------------------------|---------------------------------------|
| | All experiments | Experiments with seawater [B] | Pumping experiments with seawater [B] |
| pH _T | 0.03 | 0.80* | 0.81* |
| [HCO ₃ ⁻] | -0.16 | -0.80* | -0.81* |
| DIC | -0.18 | -0.77* | -0.80* |
| [B(OH) ₄ ⁻] ² / [CO ₃][HCO ₃] ² | 0.19 | 0.46* | 0.47* |
| [B(OH) ₄ ⁻] / [HCO ₃] | 0.33* | 0.77* | 0.76* |
| [B(OH) ₄ ⁻] / ([CO ₃ ²⁻] + [HCO ₃]) | 0.47* | 0.90* | 0.90* |
| [B(OH) ₃] | 0.55* | -0.82* | -0.83* |
| [B]/[Ca] | 0.58* | 0.38* | 0.23 |
| [B] | 0.62* | -0.41* | -0.35 |
| [B(OH) ₄ ⁻] / ΔCO ₃ ²⁻ | 0.78* | 0.70* | 0.92* |
| [B(OH) ₄ ⁻] | 0.79* | 0.82* | 0.83* |
| [B]/[HCO ₃] | 0.81* | 0.84* | 0.85* |
| [B(OH) ₄ ⁻] / [CO ₃ ²⁻] | 0.83* | 0.81* | 0.93* |
| [B]/([CO ₃ ²⁻] + [HCO ₃]) | 0.89* | 0.93* | 0.97* |
| [B]/[DIC] | 0.89* | 0.94* | 0.97* |
| [B(OH) ₄ ⁻] * [Ca ²⁺] | 0.92* | 0.82* | 0.81* |
| [B(OH) ₄ ⁻] / [CO ₃ ²⁻] ^{0.5} | 0.95* | 0.94* | 0.95* |

of the other potential relationships become significant (Table 1). For instance, [B(OH)₄⁻] / [CO₃²⁻] is highly correlated with B/Ca, especially for pumping experiments, as is [B(OH)₄⁻] / [CO₃²⁻]^{0.5}, yet these two ratios show opposite behaviors in seawater as a function of pH (Fig. 2G,H). Given the range of DIC (2.8–29 mmol/kg sw) and [B] (0.39–2.1 mmol/kg sw) among experiments (Table S2), DIC and [B] would be expected to have a greater influence on [B(OH)₄⁻] / [CO₃²⁻] and [B(OH)₄⁻] / [CO₃²⁻]^{0.5} than pH, thus a positive correlation is expected. Similarly mean [B(OH)₄⁻] / [CO₃²⁻]^{0.5} and [B]/[DIC] were highly correlated (Pearson correlation coefficient: 0.954) as would be expected given the large ranges of DIC and [B] and their consequent influence on [B(OH)₄⁻] / [CO₃²⁻]^{0.5} (e.g. Fig. 2). Since DIC is nearly equivalent to [CO₃²⁻] + [HCO₃], no separate treatment will be given of the [B]/([CO₃²⁻] + [HCO₃]) relationship. Linear least squares regression (excluding one outlier, experiment 1c) gave the following fits:

$$\text{B/Ca (mmol/mol)} = 0.0604 (\pm 0.0022) \left[\text{B(OH)}_4^- / \text{CO}_3^{2-} \right]^{0.5} + 0.0411 (\pm 0.012) \quad (4)$$

$$\text{B/Ca (mmol/mol)} = 2.88 (\pm 0.13) [\text{B}]/[\text{DIC}] + 0.085 (\pm 0.014) \quad (5)$$

where [B(OH)₄⁻], [CO₃²⁻], [B], and [DIC] are in units of μmol kg sw⁻¹, values in parentheses are 1 standard error, all parameter estimates were significant ($p \leq 0.001$, $R^2 = 0.93$ for Eq. (4), $R^2 = 0.89$ for Eq. (5)).

Although our data provide no means of assessing whether B/Ca in the aragonite precipitate depends upon solution [B(OH)₄⁻] / [CO₃²⁻]^{0.5} or [B] / [DIC], the relationship based on borate and carbonate was chosen for further investigation as CO₃²⁻ was considered to be more relevant for precipitation than total DIC (see Supplemental section S6 for calculations based on DIC as well as Ca²⁺).

Within any given experiment, the precipitate formed under a range of solution chemistry conditions. However, the range within an experiment was generally small relative to the differences among experiments. Thus K_D was assumed to be constant for a given experiment

allowing K_D values to be calculated for each individual experiment i :

$$\frac{B_i}{Ca_i} = \frac{B_i}{(\text{CO}_3)_i^{0.5}} = K_{D_i} \times \sum_{j=1}^{j=n} \frac{[\text{B(OH)}_4^-]_{i,j} \times w_{i,j}}{[\text{CO}_3^{2-}]_{i,j}^{0.5}}$$

where B/Ca is measured and is in mmol/mol, [B(OH)₄⁻] and [CO₃²⁻] are in units of μmol kg sw⁻¹, w is the fraction of total aragonite formed in time interval j as estimated from the difference in expected and measured alkalinity, i signifies an individual experiment, and j is one of n measurements taken during the course of aragonite precipitation in experiment i . Aragonite is assumed to be pure CaCO₃, thus Ca = CO₃ with activities = 1, so the exponent can be dropped for the solid phase. Calculated K_D values ranged from 0.042–0.103, with an average of 0.071 ± 0.011 sd. K_D values were correlated with a number of solution chemistry parameters (Fig. S4), but regressions with [B] and either [CO₃²⁻] or saturation state with respect to aragonite (Ω) explained much of the variance:

$$K_D = -0.0109 (\pm 0.00157) [\text{B}] - 0.001106 (\pm 0.00021) \Omega + 0.0994 (\pm 0.00432) \quad (6)$$

$$K_D = -0.01215 (\pm 0.00159) [\text{B}] - 0.0000119 (\pm 0.000002) [\text{CO}_3^{2-}] + 0.09474 (\pm 0.00323) \quad (7)$$

where [B] is in units of mmol kg sw⁻¹, and [CO₃²⁻] is in units of μmol kg sw⁻¹, with $R^2 = 0.49$, $p < 0.001$ and $R^2 = 0.53$, $p < 0.001$ for Eqs (6) and (7) respectively. Note that Ω and [CO₃²⁻] were highly correlated (Pearson correlation coefficient: 0.94).

Using Eqs. (6)–(7), the B/Ca ratio for each precipitate was predicted based on each measurement time-point. The differences between the measured and predicted B/Ca ratios showed no significant correlation with any solution chemistry parameter (see Supplemental .xls file), nor was there any significant effect of temperature, calcein, nor of organic buffering compounds (though precipitates formed in the presence of HEPES tended to have B/Ca ratios higher than predicted, while those formed in the presence of TRIS tended to be lower). Differences between measured and predicted (for both (6) and (7)) B/Ca ratios were typically <0.03 mmol/mol or 8% relative difference.

4. Discussion

How boron is incorporated into aragonite remains uncertain. Many relationships (e.g. Eqs. (1)–(3)) have been proposed to explain how B/Ca depends on solution chemistry. The wide range of solution chemistries achieved in our experiments allows us to evaluate many of the proposed relationships.

In contrast to previous work (Hemming and Hanson, 1992), we found no significant relationship between the B/Ca ratio in aragonite and the [B(OH)₄⁻]/[HCO₃]⁻ ratio in solution (Fig. 3f). Rather, our results indicate that B/Ca depends on [B(OH)₄⁻] / [CO₃²⁻]^{0.5} (Fig. 3h), suggesting that Eq. (2) represents the appropriate expression for the distribution coefficient. A dependence of B/Ca on [B(OH)₄⁻] and [CO₃²⁻] is the most likely scenario, due both to data suggesting B(OH)₄⁻ to be the primary form of B incorporated (e.g. Hemming et al., 1995; Mavromatis et al., 2015), and the involvement of CO₃²⁻ in the formation of CaCO₃ (but see Wolthers et al., 2012). For a reaction involving B(OH)₄⁻ and CO₃²⁻, a B(OH)₄⁻ can balance the charge of only 1/2 a CO₃²⁻, thus a dependence on [B(OH)₄⁻] / [CO₃²⁻]^{0.5} would be expected, consistent with our data (Fig. 3D).

Other possibilities do, however, exist. The significant correlation between B/Ca and [B(OH)₄⁻] * [Ca²⁺] could suggest the involvement of CaB(OH)₄⁺, though it could also reflect the importance of [B(OH)₄⁻] combined with a negative correlation between [CO₃²⁻] and [Ca] in a sub-set of experiments (discussed further in the supplement). Variations in [B]/[DIC] were strongly correlated with B/Ca and [B(OH)₄⁻] /

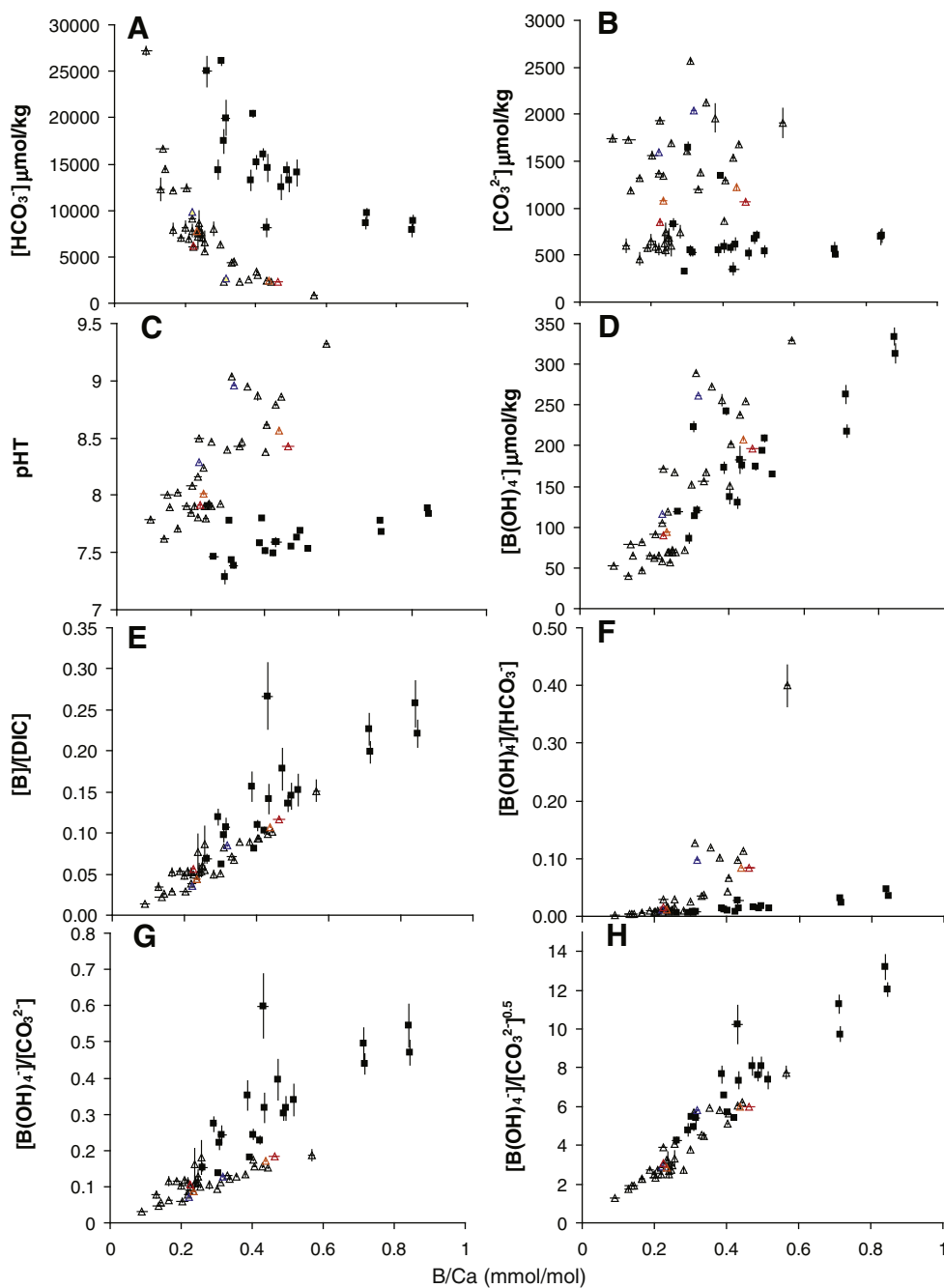


Fig. 3. Relationship between B/Ca (mmol/mol) in aragonite and various solution chemistry parameters. Units for all species in solution are $\mu\text{mol/kg}$ sw. Symbols are as described for Fig. 2.

$[\text{CO}_3^{2-}]^{0.5}$ reflecting the dependence of $[\text{B}(\text{OH})_4^-] / [\text{CO}_3^{2-}]^{0.5}$ on [B] and [DIC] combined with the pH dependencies of both B and DIC species; thus we cannot rule out the possibility of B/Ca being controlled by [B]/[DIC]. For calcite, existing work points to [B]/[DIC] and growth rate being the primary controls on B/Ca (Uchikawa et al., 2015). However, recalculating the data of Uchikawa et al. (2015) as B/Ca / $[\text{B}(\text{OH})_4^-] / [\text{CO}_3^{2-}]^{0.5}$ versus growth rate gives a very similar fit to that obtained with [B]/[DIC] ($R^2 = 0.86$ vs 0.88), again reflecting the difficulty of experimentally decoupling these parameters without simultaneously changing other chemical parameters.

4.1. Partition coefficient K_D

Using our experimental data, we calculated partition coefficients (K_D) for $[\text{B}(\text{OH})_4^-] / [\text{CO}_3^{2-}]^{0.5}$ between aragonite and solution. This

allows us to identify which factors influence B/Ca ratios in addition to the primary control of the solution $[\text{B}(\text{OH})_4^-] / [\text{CO}_3^{2-}]^{0.5}$ ratio. The K_D appears to depend upon the boron concentration and the saturation state or $[\text{CO}_3^{2-}]$ (Eqs. (6), (7), Fig. S4). A dependence upon boron concentration is consistent with previous work (Hemming et al., 1995), though our experiments likely did not cover a large enough range of [B] to fully describe this dependence (discussed below). In addition, we found a relationship between K_D and saturation state, which may reflect the influence of growth rate because aragonite crystals precipitate faster from solutions of greater supersaturation (e.g. Burton and Walter, 1987). Other studies have also suggested a growth rate influence on boron incorporation in calcite (Hobbs and Reardon, 1999; Gabitov et al., 2014; Uchikawa et al., 2015) and aragonite (Mavromatis et al., 2015). However, in contrast to the positive relationships between B/Ca and precipitation rate observed previously, we found a negative,

albeit weak, correlation between B/Ca and precipitation rate (see Supplemental .xls file for rates) or saturation state.

Several possibilities exist to explain the different signs of the effect of precipitation rate on B/Ca between our experiments and previous studies. For studies on calcite, such differences may reflect fundamental differences in how B is incorporated in calcite versus aragonite (e.g. Kitano et al., 1978; Mavromatis et al., 2015), but such an explanation cannot account for differences between our results and those of Mavromatis et al. (2015) for aragonite. However, for experiments conducted at similar [B] to ours, B/Ca data of Mavromatis et al. (2015) correlated with $[B(OH)_4^-] / [CO_3^{2-}]^{0.5}$ (calculated from Table 1 of Mavromatis et al. (2015)) and when expressed as $B/Ca/[B(OH)_4^-] / [CO_3^{2-}]^{0.5}$ their K_D values were consistently lower than those reported here (Table 2). The experiments of Mavromatis et al. (2015) were conducted at lower saturation states than those used in our study; thus such differences may reflect an effect of growth rate on B/Ca which is particularly pronounced at low supersaturation states. It should also be noted that the experiments of Mavromatis et al. (2015) were not conducted using seawater, so the ionic composition of the fluid may influence partitioning (e.g. Kitano et al., 1978).

Alternatively, the expression used for the partition coefficient may play some role in the observed correlations between B/Ca and precipitation rate. Since K_D could be fit almost equally well using saturation state (Eq. (6)) or $[CO_3^{2-}]$ (Eq. (7)), any dependence of K_D on Ω may reflect the dependency of Ω on $[CO_3^{2-}]$. Thus the dependence of K_D on $[CO_3^{2-}]$ may not reflect a growth rate effect associated with Ω , instead it could indicate that Eq. (2) does not fully describe the exchange reaction and that the relationship between $B(OH)_4^-$ and $[CO_3^{2-}]$ deviates from the 1: 0.5 ratio used. Although a few of our experiments were conducted at different $[CO_3^{2-}]$ but similar Ω , and vice-versa, and thus could potentially be used to determine whether $[CO_3^{2-}]$ or Ω drives partitioning, no clear pattern was observed.

Any influence of temperature or various additives was small relative to other sources of variability as no significant effects were detected, which contrasts with some studies of natural samples as well as one study of synthetic aragonite which point to a temperature effect (Sinclair et al., 1998; Wara et al., 2003; Yu et al., 2007; Mavromatis et al., 2015). It should be noted that because temperature influences saturation state, B and DIC speciation, such effects, if not corrected for, could give rise to an apparent temperature dependency for B/Ca. In the case of Mavromatis et al. (2015), the K_D expression used was based on [B] and not $[B(OH)_4^-]$, thus changes in boron speciation with temperature could account for the temperature influence; recalculating their data per Eq. (2) however shows no evidence for a temperature effect on K_D based on the same data points.

4.2. Prior K_D estimates

Although the partitioning of B into aragonite has previously been investigated (Kitano et al., 1978; Hemming et al., 1995; Mavromatis et al., 2015), only the study of Mavromatis et al. (2015) characterized carbonate chemistry, thus making it difficult to compare our results with much of the prior work. The experiments of Kitano et al. (1978) were similar to our degassing experiments, but carbonate chemistry was not reported during precipitation; given the range of carbonate chemistry values

which can potentially be generated during such an experiment we cannot satisfactorily estimate carbonate chemistry for these experiments. Hemming and Hanson (1992) estimated $K_D \sim 0.012$ via Eq. (1) (or 12 to be consistent with expressing B/Ca as mmol/mol as used elsewhere in our paper) for biogenic calcium carbonate samples, which is well within the range estimated in our study (Table 2). For the experiments of Hemming et al. (1995) detailed carbonate chemistry measurements are lacking, however using their measured pH and calculated $[Ca^{2+}]$, and our observation that precipitation typically starts near $\Omega = 20$, we can make rough estimates of the relevant parameters: $[HCO_3^-] = 1000 \mu\text{mol/kg}$, $[CO_3^{2-}] = 100 \mu\text{mol/kg}$, and, depending upon the experiment, $[B(OH)_4^-] = 0.012, 0.107, \text{ or } 0.78 \text{ mmol/kg}$. Using these values, we can estimate K_D via Eqs (1) and (2) (Table 2). Despite experimental differences, the K_D estimates based on Hemming et al. (1995) fall within the range of values found in the current study. Further, if we use Eq. (6) to estimate K_D using the above constraints, we would predict a K_D range of 0.08 to 0.04, and with Eq. (7): 0.09 to 0.05. At the boron concentration closest to seawater used by Hemming et al. (1995), the difference between K_D predicted minus that calculated is -0.001 for Eq. (6), and 0.01 for Eq. (7). The range of boron concentrations used by Hemming et al. (1995) includes concentrations well below ($\sim 13\%$ of seawater values) those used in the current study, and at [B] well below seawater values, both Eqs. (6) and (7) underestimate K_D . The study of Mavromatis et al. (2015) included boron concentrations ranging from near seawater values to $\sim 20 \times$ seawater values. At high [B], both Eqs. (6) and (7) predict negative K_D values for the Mavromatis et al. (2015) data, indicating that neither equation can be reliably extrapolated far beyond the concentration range used for fitting the equations. Within the range for which [B] was similar, Eqs. (6) and (7) both predicted K_D values higher (up to a factor of $10 \times$) than those calculated from Mavromatis et al. (2015). The highest Ω (5.8) used by Mavromatis et al. (2015) was below the lowest values used in the current study, so a growth rate or saturation state influence on K_D could be involved. Our experiment 1c, which precipitated at a lower Ω than any of our other experiments had the lowest K_D , consistent with a positive effect of growth rate at low Ω values.

The agreement between K_D estimates both across the diverse conditions used in the current study and for independent studies, suggests that Eqs. (6) and (7) provide reasonable estimates of K_D over a wide range of conditions, except at $[B] \ll \text{seawater}$, $[B] \gg \text{seawater}$, and $\Omega < \sim 9$.

4.3. Nernst partition coefficient

An alternative means of expressing partitioning is to use the single element or Nernst partition coefficient (D_B), which is expressed as the ratio of the mass percent B in the solid relative to the mass percent in solution (e.g. Gaetani and Cohen, 2006). The use of Nernst partition coefficients allows different studies to be compared as prior studies have generally provided the necessary data. Values for Nernst partition coefficients are dependent upon the specific experimental conditions (temperature, pH, competing species, etc) (e.g. McIntire, 1963), as they do not necessarily take into account speciation changes or other factors influencing incorporation, thus comparisons should be interpreted with this in mind. Values for D_B were calculated for each experiment as described for K_D calculations, and are summarized in Table 3 along with those of other studies. D_B values from the current study were strongly correlated with pH_T (Pearson correlation coefficient: 0.888), as well as with a wide range of other solution chemistry parameters (Fig. 4), likely reflecting changes in boron and carbon speciation with pH. The following equations described much of the variance in D_B values:

$$D_B = 8.215 (\pm 0.40) pH_T - 0.297 (\pm 0.035)\Omega - 55.69 (\pm 2.81) \quad (8)$$

Table 2

K_D values calculated using different equations for the current study and the studies of Hemming et al. (1995) and Mavromatis et al. (2015). See discussion for further details on the calculations. Note that K_D values expressed here are for expressing B/Ca as mmol/mol. For the current study, mean values are expressed ± 1 standard deviation.

| Study | Eq. (1) K_D | Eq. (2) K_D |
|--------------------|----------------------------------|-------------------------------------|
| Hemming B) | 4.5 (37 ppm B) – 10 (0.59 ppm B) | 0.04 (37 ppm B) – 0.1 (0.59 ppm B) |
| Mavromatis Current | 0.3–40 | 0.0003–0.03 |
| | 1.4–52, mean 23 \pm 14 | 0.042–0.103, mean 0.071 \pm 0.011 |

Table 3

Nernst coefficients (D_B) estimated from different studies. Note that for estimating D_B for the Hemming and Hanson (1992) study, it was assumed that the biogenic CaCO_3 samples precipitated from a solution with 4.676 ppm B, all other studies represent synthetic aragonites and [B] was specified in the study.

| Study | D_B |
|---------------------------|------------------------------|
| Kitano et al. (1978) | ~0.53–1.5 |
| Hemming and Hanson (1992) | 2–15 |
| Hemming et al. (1995) | 10.2–22.8 |
| Mavromatis et al. (2015) | 0.07–9 |
| Current | 1.5–14.4, mean 5.4 ± 3.0 |

$$D_B = 7.954 (\pm 0.378) \text{pH}_T - 0.267 (\pm 0.034) \Omega + 0.124 (\pm 0.038) T - 57.3 (\pm 2.6) \quad (9)$$

$$D_B = 7.429 (\pm 0.423) \text{pH}_T - 0.260 (\pm 0.033) \Omega + 0.114 (\pm 0.037) T - 0.491 (\pm 0.203) [\text{B}] - 52.5 (\pm 3.2) \quad (10)$$

where Ω is the saturation state with respect to aragonite, pH_T is the pH on the total scale, T is temperature in Celsius. All parameter estimates were significant at the $p < 0.05$ level, those for the constant, pH and saturation state were all highly significant ($p < 0.001$), $R^2 = 0.9$, 0.92, and 0.93 for Eqs. (8), (9), and (10) respectively. Note that D_B depends on factors such as pH and temperature, whereas the K_D values did not, likely reflecting changes in speciation of B and DIC as a function of pH and temperature which were taken into account when calculating K_D .

Differences between the predicted (using Eq. (10)) and measured solid composition were not strongly correlated with any solution chemistry parameter, though there was a weak positive correlation with growth rate and with salinity; no significant effects of organic buffers

were detected. Relative differences between measured and predicted values were generally less than 16%.

Our estimates of D_B agree well with existing values – our experimental range covers the range estimated for natural aragonite (Table 3). Our highest values overlap the lower estimates of Hemming et al. (1995); for the two highest [B] used by Hemming et al., their values are only slightly higher than some of our estimates at similar [B]. Estimates of D_B from Kitano et al. (1978) and Mavromatis et al. (2015), though below those of Hemming et al. (1995), also overlap our values, with their estimates for their lowest [B] being similar to our values at similar [B]. Although both the D_B values of Kitano et al. (1978) and Hemming et al. (1995) overlap ours, the values in the two studies do not overlap (Table 3). This lack of agreement between these two previous studies likely reflects differences in the carbonate chemistry during aragonite precipitation. In the experiments performed by Hemming et al. (1995), CO_2 diffusion into the solution controlled precipitation, thus aragonite was formed under low [DIC] and low $[\text{CO}_3^{2-}]$ conditions, with $[\text{CO}_3^{2-}]$ likely lower than any of our experiments or those of Kitano et al. (1978). Such low $[\text{CO}_3^{2-}]$ conditions would in-turn lead to an increase in the $[\text{B}(\text{OH})_4^-] / [\text{CO}_3^{2-}]^{0.5}$ ratio relative to other studies, thus a higher percentage of solution B would be expected to be incorporated into the aragonite, consistent with high D_B estimates (Table 3). In contrast, Kitano et al. (1978) used CO_2 degassing experiments, with much lower $[\text{Ca}^{2+}]$ and higher [DIC]. Although insufficient detail is given to estimate $[\text{CO}_3^{2-}]$ for these experiments, concentrations were likely much higher than those of Hemming et al. (1995), potentially similar to ours, consistent with similar D_B estimates. However, Kitano et al. (1978) also used boron concentrations much higher than those used in the current study, and high [B] resulted in lower D_B values.

The pattern of lower D_B or K_D values at higher [B] is consistent across studies.

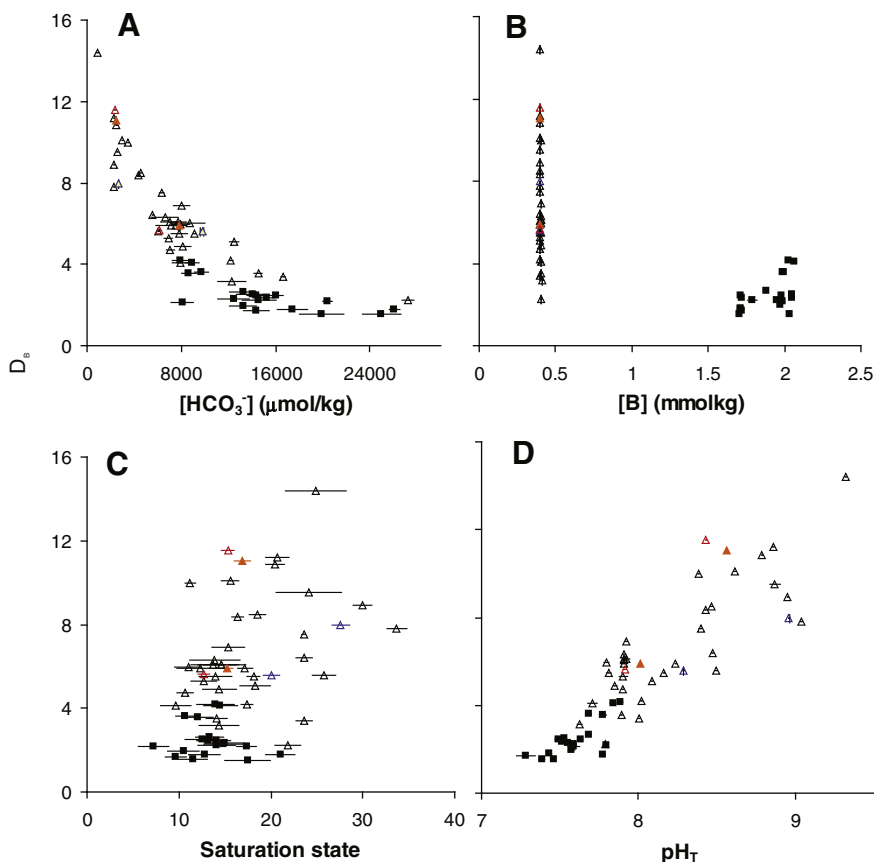


Fig. 4. Relationship between the Nernst partition coefficient (D_B) and various solution chemistry parameters. Symbols are as described for Fig. 2.

Such observations have previously been suggested to be due to saturating defect sites at which incorporation is more favorable at relatively low concentrations leaving only structural sites for further substitution (Hemming et al., 1995). Changes in boron speciation may also occur at high concentrations (e.g. Williams and Strack, 1966) which could further affect partitioning. It should also be noted that boron can influence the growth of crystals along different axes (Ruiz-Agudo et al., 2012) and solution chemistry influences surface charging which may further influence B incorporation (Hobbs and Reardon, 1999). Although our data provide insight into the controls on B incorporation into aragonite in terms of bulk solution influences, there remains considerable research to be done to understand the detailed mechanisms of B incorporation, particularly with regards to the reactions and molecular rearrangements occurring near the crystal surface, which ultimately control B incorporation and B/Ca ratios.

4.4. Environmental proxies

Although our results show patterns consistent with some studies of biologically formed calcium carbonates e.g. $[B(OH)_4^-]/\Delta CO_3^{2-}$ was strongly correlated with B/Ca (Table 1; Yu and Elderfield, 2007), such results cannot be directly compared. Here we directly measure the chemistry during precipitation and thus correlate B/Ca in aragonite to the chemistry in the solution from which that aragonite formed, whereas studies of material in the natural environment usually measure seawater chemistry, not the chemistry of the solution from which precipitation occurs, and thus make an assumption about the link between seawater chemistry and the chemistry of the fluid responsible for precipitation. Biologically formed aragonite is often formed from a solution substantially modified from seawater, for instance, in corals aragonite growth occurs from a solution in which pH and $[CO_3^{2-}]$ are elevated relative to the surrounding seawater (e.g. Al-Horani et al., 2003; McCulloch et al., 2012; DeCarlo et al., 2015; Cai et al., 2016). Similarities in relationships between B/Ca and seawater chemistry reported for biological samples and relationships between B/Ca and directly measured solution chemistry in synthetic precipitates suggests that variations in seawater chemistry affect the internal calcifying environment of calcifying organisms. With the relationships described here for synthetic aragonite, B/Ca holds potential as a proxy to determine how the chemistry of the internal calcifying environment of biomineralizing organisms is linked to the external environment. With this framework, B/Ca ratios of the shells and skeletons of calcifying organisms can improve our understanding of how environmental conditions are recorded in biogenic aragonite.

5. Summary

The B/Ca ratio in aragonite appears to be primarily a function of $[B(OH)_4^-] / [CO_3^{2-}]^{0.5}$ in the solution from which aragonite growth occurs, with possible influences of [B] and saturation state/ $[CO_3^{2-}]$. For aragonites formed from seawater-like solutions, [B] can be estimated from salinity, and since pH can be estimated from boron isotopes (e.g. Trotter et al., 2011), $[B(OH)_4^-]$ can be calculated (assuming T is known), thus the remaining variables influencing B/Ca are $[CO_3^{2-}]$ and potentially $[Ca^{2+}]$. B/Ca can be used to estimate $[CO_3^{2-}]$, thus allowing the full carbonate chemistry under which the aragonite formed to be estimated. If it can be shown that the solution chemistry from which aragonite precipitates in a particular organism varies in a predictable way with seawater chemistry, it may further be possible to use B/Ca in biogenic carbonates to infer past seawater conditions.

Acknowledgments

We wish to thank the following for invaluable assistance with this study: R. Belastock, E. Bonk, A. Cohen, D. McCorkle, M. Sulanowska, D. Wellwood, and S. White at Woods Hole Oceanographic Institution; J.P.

D'Olivo Cordero, R. Hart, H. Oskierski, K. Rankenburg, K. Tanaka and J. Trotter at the University of Western Australia. This work was supported by the Australian Research Council (ARC) Centre of Excellence for Coral Reef Studies. Research conducted at WHOI was supported by NSF grant OCE-1338320. M.H. was supported by an ARC Super Science Fellowship and an NSF International Postdoctoral Fellowship. T.D. was supported by a NSF Graduate Research Fellowship. M.M. was supported by a Western Australian Premiers Fellowship and an ARC Laureate Fellowship. The authors acknowledge the facilities, and the scientific and technical assistance of the Australian Microscopy and Microanalysis Research Facility at The University of Western Australia Centre for Microscopy, Characterization & Analysis, a facility funded by the University, State and Commonwealth Governments.

Appendix A. Supplementary data

Supplementary data to this article can be found online at <http://dx.doi.org/10.1016/j.chemgeo.2016.05.007>.

References

- Al-Horani, F.A., Al-Moghrabi, S.M., de Beer, D., 2003. The mechanism of calcification and its relation to photosynthesis and respiration in the scleractinian coral *Galaxea fascicularis*. *Mar. Biol.* 142, 419–426.
- Allen KA, Hönisch B, Eggins SM, Yu J, Spero HJ, Elderfield H. 2011. Controls on boron incorporation in cultured tests of the planktic foraminifer *Orbulina universa*. *Earth Planet. Sci. Lett.* 309:291–301 doi: <http://dx.doi.org/http://dx.doi.org/10.1016/j.epsl.2011.07.010>.
- Allen KA, Hönisch B, Eggins SM, Rosenthal Y. 2012. Environmental controls on B/Ca in calcite tests of the tropical planktic foraminifer species *Globigerinoides ruber* and *Globigerinoides sacculifer*. *Earth Planet. Sci. Lett.* 351–352:270–280 doi: <http://dx.doi.org/http://dx.doi.org/10.1016/j.epsl.2012.07.004>.
- Allison, N., Cohen, I., Finch, A.A., Erez, J., Tudhope, A.W., 2014. Corals concentrate dissolved inorganic carbon to facilitate calcification. *Nat. Commun.* 5:10.1038/ncomms6741.
- Babila TL, Rosenthal Y, Conte MH. 2014. Evaluation of the biogeochemical controls on B/Ca of *Globigerinoides ruber* white from the oceanic flux program, Bermuda. *Earth Planet. Sci. Lett.* 404:67–76 doi: <http://dx.doi.org/http://dx.doi.org/10.1016/j.epsl.2014.05.053>.
- Burton, E.A., Walter, L.M., 1987. Relative precipitation rates of aragonite and Mg calcite from seawater: temperature or carbonate ion control? *Geology* 15, 111–114.
- Cai, W.-J., Ma, Y., Hopkinson, B.M., Grotto, A.G., Warner, M.E., Ding, Q., Hu, X., Yuan, X., Schoepf, V., Xu, H., Han, C., Melman, T., Hoadley, K.D., Pettay, D.T., Matsui, Y., Baumann, J.H., Levas, S., Ying, Y., Wang, Y., 2016. Microelectrode characterization of coral daytime interior pH and carbonate chemistry. *Nat. Commun.* 7, 11144.
- Culbertson, C., Pytkowicz, R.M., 1968. Effect of pressure on carbonic acid, boric acid, and the pH in seawater. *Limnol. Oceanogr.* 13, 403–417.
- de Nooijer LJ, Spero HJ, Erez J, Bijma J, Reichert GJ. 2014. Biomineralization in perforate foraminifera. *Earth Sci. Rev.* 135:48–58 doi: <http://dx.doi.org/http://dx.doi.org/10.1016/j.earscirev.2014.03.013>.
- DeCarlo TM, Gaetani GA, Holcomb M, Cohen AL. 2015. Experimental determination of factors controlling U/Ca of aragonite precipitated from seawater: implications for interpreting coral skeleton. *Geochim. Cosmochim. Acta* 162:151–165 doi: <http://dx.doi.org/http://dx.doi.org/10.1016/j.gca.2015.04.016>.
- Dickson, A.G., 1990. Thermodynamics of the dissociation of boric acid in synthetic seawater from 273.15 to 318.15 K. *Deep-Sea Res.* 37, 755–766.
- Dissard, D., Nehrke, G., Reichert, G.J., Nouet, J., Bijma, J., 2009. Effect of the fluorescent indicator calcein on Mg and Sr incorporation into foraminiferal calcite. *Geochim. Geophys. Geosyst.* 10, Q11001. <http://dx.doi.org/10.1029/2009GC002417>.
- Douville, E., Paterne, M., Cabioch, G., Louvat, P., Gaillardet, J., Juillet-Leclerc, A., Ayliffe, L., 2010. Abrupt sea surface pH change at the end of the younger Dryas in the central sub-equatorial Pacific inferred from boron isotope abundance in corals (<i>Porites</i>). *Biogeosciences* 7, 2445–2459. <http://dx.doi.org/10.5194/bg-7-2445-2010>.
- Foster, G.L., 2008. Seawater pH, pCO₂ and [CO₂–3] variations in the Caribbean Sea over the last 170 kyr: a boron isotope and B/Ca study of planktic foraminifera. *Earth Planet. Sci. Lett.* 271, 254–266. <http://dx.doi.org/10.1016/j.epsl.2008.04.015>.
- Gabitov, R.I., Schmitt, A.K., Rosner, M., McKeegan, K.D., Gaetani, G.A., Cohen, A.L., Watson, E.B., Harrison, T.M., 2011. In situ ⁷Li, Li/Ca, and Mg/Ca analyses of synthetic aragonites. *Geochim. Geophys. Geosyst.* <http://dx.doi.org/10.1029/2010gc003322>.
- Gabitov, R.I., Rollion-Bard, C., Tripathi, A., Sadekov, A., 2014. In situ study of boron partitioning between calcite and fluid at different crystal growth rates. *Geochim. Cosmochim. Acta* 137, 81–92. <http://dx.doi.org/10.1016/j.gca.2014.04.014>.
- Gaetani, G.A., Cohen, A.L., 2006. Element partitioning during precipitation of aragonite from seawater: a framework for understanding paleoproxies. *Geochim. Cosmochim. Acta* 70, 4617–4634.
- Hain, M.P., Sigman, D.M., Higgins, J.A., Haug, G.H., 2015. The effects of secular calcium and magnesium concentration changes on the thermodynamics of seawater acid/base chemistry: implications for eocene and cretaceous ocean carbon chemistry and buffering. *Glob. Biogeochem. Cycles* 29 2014GB004986 [10.1002/2014gb004986](https://doi.org/10.1002/2014gb004986).
- Hathorne, E.C., Gagnon, A., Felis, T., Adkins, J., Asami, R., Boer, W., Caillon, N., Case, D., KM, C., Douville, E., deMenocal, P., Eisenhauer, A., Garbe-Schönberg, C.D., Geibert, W.,

- Goldstein, S., Huguen, K., Inoue, M., Kawahata, H., Kölling, M., Le Cornec, F., Linsley, B.K., McGregor, H.V., Montagna, P., Nurhati, I.S., Quinn, T.M., Raddatz, J., Rebaubier, H., Robinson, L., Sadekov, A., Sherrell, R., Sinclair, D., Tudhope, A.W., Wei, G., Wong, H., Wu, H.C., You, C.-F., 2013. Inter-laboratory study for coral Sr/Ca and other element/Ca ratio measurements. *Geochem. Geophys. Geosyst.* n/a-n/a 10.1002/ggge.20230.
- He M, Xiao Y, Jin Z, Liu W, Ma Y, Zhang Y, Luo C. 2013. Quantification of boron incorporation into synthetic calcite under controlled pH and temperature conditions using a differential solubility technique. *Chem. Geol.* 337–338:67–74 doi: <http://dx.doi.org/10.1016/j.chemgeo.2012.11.013>.
- Hemming NG, Hanson GN. 1992. Boron isotopic composition and concentration in modern marine carbonates. *Geochim. Cosmochim. Acta* 56:537–543 doi: [http://dx.doi.org/10.1016/0016-7037\(92\)90151-8](http://dx.doi.org/10.1016/0016-7037(92)90151-8).
- Hemming NG, Reeder RJ, Hanson GN. 1995. Mineral-fluid partitioning and isotopic fractionation of boron in synthetic calcium carbonate. *Geochim. Cosmochim. Acta* 59:371–379 doi: [http://dx.doi.org/10.1016/0016-7037\(95\)00288-B](http://dx.doi.org/10.1016/0016-7037(95)00288-B).
- Henehan, M.J., Rae, J.W.B., Foster, G.L., Erez, J., Prentice, K.C., Kucera, M., Bostock, H.C., Martínez-Botí, M.A., Milton, J.A., Wilson, P.A., Marshall, B.J., Elliott, T., 2013. Calibration of the boron isotope proxy in the planktonic foraminifera *Globigerinoides ruber* for use in palaeo-CO₂ reconstruction. *Earth Planet. Sci. Lett.* 364, 111–122. <http://dx.doi.org/10.1016/j.epsl.2012.12.029>.
- Henehan, M.J., Foster, G.L., Rae, J.W.B., Prentice, K.C., Erez, J., Bostock, H.C., Marshall, B.J., Wilson, P.A., 2015. Evaluating the utility of B/Ca ratios in planktic foraminifera as a proxy for the carbonate system: a case study of *Globigerinoides ruber*. *Geochem. Geophys. Geosyst.* 16, 1052–1069. <http://dx.doi.org/10.1002/2014gc005514>.
- Hobbs, M.Y., Reardon, E.J., 1999. Effect of pH on boron coprecipitation by calcite: further evidence for nonequilibrium partitioning of trace elements. *Geochim. Cosmochim. Acta* 63, 1013–1021.
- Holcomb, M., Cohen, A.L., Gabitov, R.I., Hutter, J.L., 2009. Compositional and morphological features of aragonite precipitated experimentally from seawater and biogenically by corals. *Geochim. Cosmochim. Acta* 73, 4166–4179. <http://dx.doi.org/10.1016/j.gca.2009.04.015>.
- Kaczmarek, K., Langer, G., Nehrke, G., Horn, I., Misra, S., Janse, M., Bijma, J., 2015. Boron incorporation in the foraminifer *Ammonia lessona* under a decoupled carbonate chemistry. *Biogeosciences* 12, 1753–1763. <http://dx.doi.org/10.5194/bg-12-1753-2015>.
- Kinsman, D.J.J., Holland, H.D., 1969. The co-precipitation of cations with CaCO₃-IV. The co-precipitation of Sr²⁺ with aragonite between 16 and 96°C. *Geochim. Cosmochim. Acta* 33, 1–17.
- Kitano, Y., Okumura, M., Idogaki, M., 1978. Coprecipitation of borate-boron with calcium carbonate. *Geochem. J.* 12, 183–189.
- Klochko, K., Kaufman, A.J., Yao, W., Byrne, R.H., Tossell, J.A., 2006. Experimental measurement of boron isotope fractionation in seawater. *Earth Planet. Sci. Lett.* 248, 276–285. <http://dx.doi.org/10.1016/j.epsl.2006.05.034>.
- Klochko, K., Cody, G.D., Tossell, J.A., Dera, P., Kaufman, A.J., 2009. Re-evaluating boron speciation in biogenic calcite and aragonite using 11B MAS NMR. *Geochim. Cosmochim. Acta* 73, 1890–1900. <http://dx.doi.org/10.1016/j.gca.2009.01.002>.
- Mass, T., Drake, J.L., Haramaty, L., Kim, J.D., Zelzion, E., Bhattacharya, D., Falkowski, P.G., 2013. Cloning and characterization of four novel coral acid-rich proteins that precipitate carbonates in vitro. *Curr. Biol.* 23, 1126–1131. <http://dx.doi.org/10.1016/j.cub.2013.05.007>.
- Mavromatis, V., Montouillout, V., Noireaux, J., Gaillardet, J., Schott, J., 2015. Characterization of boron incorporation and speciation in calcite and aragonite from co-precipitation experiments under controlled pH, temperature and precipitation rate. *Geochim. Cosmochim. Acta* 150, 299–313.
- McCulloch, M., Falter, J., Trotter, J., Montagna, P., 2012. Coral resilience to ocean acidification and global warming through pH up-regulation. *Nat. Clim. Chang.* 2, 623–627.
- McIntire, W.L., 1963. Trace element partition coefficients - a review of theory and applications to geology. *Geochim. Cosmochim. Acta* 27, 1209–1264.
- Ni, Y., Foster, G.L., Bailey, T., Elliott, T., Schmidt, D.N., Pearson, P., Haley, B., Coath, C., 2007. A core top assessment of proxies for the ocean carbonate system in surface-dwelling foraminifera. *Paleoceanography* 22. <http://dx.doi.org/10.1029/2006pa001337> n/a-n/a.
- Pearson, P.N., Palmer, M.R., 1999. Middle eocene seawater pH and atmospheric carbon dioxide concentrations. *Science* 284, 1824–1826. <http://dx.doi.org/10.1126/science.284.5421.1824>.
- Pelejero, C., Calvo, E., McCulloch, M.T., Marshall, J.F., Gagan, M.K., Lough, J.M., Opdyke, B.N., 2005. Preindustrial to modern interdecadal variability in coral reef pH. *Science* 309, 2204–2207.
- Penman, D.E., Hönisch, B., Rasbury, E.T., Hemming, N.G., Spero, H.J., 2013. Boron, carbon, and oxygen isotopic composition of brachiopod shells: intra-shell variability, controls, and potential as a paleo-pH recorder. *Chem. Geol.* 340, 32–39. <http://dx.doi.org/10.1016/j.chemgeo.2012.11.016>.
- Rae, J.W.B., Foster, G.L., Schmidt, D.N., Elliott, T., 2011. Boron isotopes and B/Ca in benthic foraminifera: proxies for the deep ocean carbonate system. *Earth Planet. Sci. Lett.* 302, 403–413. <http://dx.doi.org/10.1016/j.epsl.2010.12.034>.
- Rollion-Bard, C., Blamart, D., Trebosch, J., Tricot, G., Mussi, A., Cuif, J.-P., 2011. Boron isotopes as pH proxy: a new look at boron speciation in deep-sea corals using 11B MAS NMR and EELS. *Geochim. Cosmochim. Acta* 75, 1003–1012. <http://dx.doi.org/10.1016/j.gca.2010.11.023>.
- Ruiz-Agudo, E., Putnis, C.V., Kowacz, M., Ortega-Huertás, M., Putnis, A., 2012. Boron incorporation into calcite during growth: implications for the use of boron in carbonates as a pH proxy. *Earth Planet. Sci. Lett.* 345–348, 9–17. <http://dx.doi.org/10.1016/j.epsl.2012.06.032>.
- Sanyal, A., Hemming, N.G., Broecker, W.S., Lea, D.W., Spero, H.J., Hanson, G.N., 1996. Oceanic pH control on the boron isotopic composition of foraminifera: evidence from culture experiments. *Paleoceanography* 11, 513–517. <http://dx.doi.org/10.1029/96pa01858>.
- Sanyal, A., Nugent, M., Reeder, R.J., Bigma, J., 2000. Seawater pH control on the boron isotopic composition of calcite: evidence from inorganic calcite precipitation experiments. *Geochim. Cosmochim. Acta* 64, 1551–1555.
- Sen, S., Stebbins, J.F., Hemming, N.G., Ghosh, B., 1994. Coordination environments of B impurities in calcite and aragonite polymorphs: a 11B MAS NMR study. *Am. Mineral.* 79, 819–825.
- Sinclair, D.J., Kinsley, L.P.J., McCulloch, M.T., 1998. High resolution analysis of trace elements in corals by laser ablation ICP-MS. *Geochim. Cosmochim. Acta* 62, 1889–1901.
- Tripati AK, Roberts CD, Eagle RA, Li G. 2011. A 20 million year record of planktic foraminiferal B/Ca ratios: systematics and uncertainties in pCO₂ reconstructions. *Geochim. Cosmochim. Acta* 75:2582–2610 doi: <http://dx.doi.org/10.1016/j.gca.2011.01.018>.
- Trotter, J., Montagna, P., McCulloch, M., Silenzi, S., Reynaud, S., Mortimer, G., Martin, S., Ferrier-Pagès, C., Gattuso, J.-P., Rodolfo-Metalpa, R., 2011. Quantifying the pH 'vital effect' in the temperate zooxanthellate coral *Cladocora caespitosa*: validation of the boron seawater pH proxy. *Earth Planet. Sci. Lett.* 303, 163–173. <http://dx.doi.org/10.1016/j.epsl.2011.01.030>.
- Uchikawa, J., Penman, D.E., Zachos, J.C., Zeebe, R.E., 2015. Experimental evidence for kinetic effects on B/Ca in synthetic calcite: Implications for potential B(OH)₄⁻ and B(OH)₃ incorporation. *Geochim. Cosmochim. Acta* 150, 171–191. <http://dx.doi.org/10.1016/j.gca.2014.11.022>.
- van Heuven, S., Pierrot, D., Lewis, E., Wallace, D.W.R., 2009. MATLAB Program developed for CO₂ system calculations. ORNL/CDIAC-105b. Carbon Dioxide Information Analysis Center, Oak Ridge National Laboratory, U.S. Department of Energy, Oak Ridge, TN.
- Venn, A.A., Tambutte, E., Holcomb, M., Laurent, J., Allemand, D., Tambutte, S., 2013. Impact of seawater acidification on pH at the tissue-skeleton interface and calcification in reef corals. *Proc. Natl. Acad. Sci. U. S. A.* 110, 1634–1639. <http://dx.doi.org/10.1073/pnas.1216153110>.
- Wang, Z., Hu, P., Gaetani, G., Liu, C., Saenger, C., Cohen, A., Hart, S., 2013. Experimental calibration of Mg isotope fractionation between aragonite and seawater. *Geochim. Cosmochim. Acta* 102, 113–123. <http://dx.doi.org/10.1016/j.gca.2012.10.022>.
- Wara, M.W., Delaney, M.L., Bullen, T.D., Ravelo, A.C., 2003. Possible roles of pH, temperature, and partial dissolution in determining boron concentration and isotopic composition in planktonic foraminifera. *Paleoceanography* 18. <http://dx.doi.org/10.1029/2002pa000797> n/a-n/a.
- Williams, P.M., Strack, P.M., 1966. Complexes of boric acid with organic cis-diols in seawater. *Limnol. Oceanogr.* 11, 401–404.
- Wolthers, M., Nehrke, G., Gustafsson, J.P., Van Cappellen, P., 2012. Calcite growth kinetics: modeling the effect of solution stoichiometry. *Geochim. Cosmochim. Acta* 77:121–134 doi: <http://dx.doi.org/10.1016/j.gca.2011.11.003>.
- Xiao, Y., Li, H., Liu, W., Wang, X., Jiang, S., 2008. Boron isotopic fractionation in laboratory inorganic carbonate precipitation: evidence for the incorporation of B(OH)₃ into carbonate. *Sci. China Ser. D Earth Sci.* 51, 1776–1785. <http://dx.doi.org/10.1007/s11430-008-0144-y>.
- Yu, J., Elderfield, H., 2007. Benthic foraminiferal B/Ca ratios reflect deep water carbonate saturation state. *Earth Planet. Sci. Lett.* 258, 73–86. <http://dx.doi.org/10.1016/j.epsl.2007.03.025>.
- Yu, J., Elderfield, H., Hönisch, B., 2007. B/Ca in planktonic foraminifera as a proxy for surface seawater pH. *Paleoceanography* 22. <http://dx.doi.org/10.1029/2006pa001347> n/a-n/a.